Digital Cancellation of Passive Intermodulation: Method, Complexity and Measurements

Muhammad Zeeshan Waheed[†*], Dani Korpi[‡], Adnan Kiayani[*], Lauri Anttila[*], and Mikko Valkama[*]
[*]Tampere University, Dept. Electrical Engineering, Tampere, Finland
[†]Nokia Mobile Networks, Finland; [‡]Nokia Bell Labs, Finland;
Contact email: mikko.valkama@tuni.fi

***Abstract*—This paper addresses digital cancellation of passive intermodulation (PIM) products in simultaneous transmit-receive systems, with specific emphasis on frequency-division duplexing (FDD) based LTE and 5G New Radio (NR) networks. Building on mathematical modeling of the passive intermodulation, a computationally efficient digital cancellation and associated parameter learning solutions are derived and presented. The performance of the method is analyzed through interband carrier aggregation based RF measurements at LTE/NR bands 1 and 3. The measurement results show that the proposed canceller can efficiently cancel the PIM products towards the receiver noise floor. Additionally, the proposed canceller is shown to be of substantially lower complexity compared to the reference methods.**

***Index Terms*—5G NR, LTE, carrier aggregation, radio coexistence, flexible duplex, frequency division duplexing, nonlinear distortion, passive intermodulation.**

I. Introduction

Coexisting and simultaneously operating radio transmitters and receivers are known to be subject to interference challenges [1]. In this paper, we focus on the possible interference of cellular transmitter to cellular receiver in frequency-division duplexing (FDD) based LTE and 5G NR systems and devices. Specifically, as identified in [2], [3], the utilization of carrier aggregation (CA) can lead to challenging self-interference scenarios where intermodulation of the transmit carriers lands directly at one of the own receive bands. Good examples of such cases at the user equipment (UE) side are, e.g., combinations of the LTE/NR bands 1 and 3, or bands 3 and 8 [2]. While band-specific power amplifiers (PAs) relax the problem to certain extent, the passive radio frequency (RF) front-end components, such as switches, diplexers and multiplexers, can be another major source of intermodulation, commonly known as passive intermodulation (PIM) [1], [4]–[6].

The self-interference problem in FDD radio transceivers can potentially be avoided or reduced through a number of approaches. These include, e.g., reducing the transmit power level, known as the maximum power reduction (MPR), or alternatively relaxing the receiver reference sensitivity requirements, commonly referred to as the maximum sensitivity degradation (MSD), in the context of LTE and NR UEs. Another option is to employ expensive high-quality RF components with good linearity characteristics in order to avoid intermodulation. However, these approaches have a negative impact on the uplink (MPR) or downlink (MSD) coverage and throughput, or on the overall radio implementation cost.

Digital cancellation techniques have recently been proposed as an alternative to resolving the self-interference problem in FDD radio transceivers, see, e.g., [4], [5], [6]. In this context, the majority of the works build on polynomial or memory polynomial like linear-in-parameters methods, combined with traditional least-squares (LS), recursive least-squares (RLS), or least mean squares (LMS) type parameter learning schemes. Additionally, in [6], it was recognized that also the band-specific power amplifers and their nonlinear characteristics can contribute to the exact PIM samples, the overall system being a challenging cascaded set of multiple nonlinearities. In such cases, particularly with both memory and nonlinearities in the individual PAs, the complexity of the effective linear in parameters model and the corresponding cancellers largely increases [4]–[6].

In this paper, we present a novel reduced-complexity digital PIM cancellation solution together with novel self-orthogonalizing decoupled parameter learning rules, for suppressing the self-interference stemming from coexisting PA and PIM nonlinearities. The performance of the proposed cancellation technique is evaluated and demonstrated through practical RF measurements adopting interband carrier aggregation at LTE/NR bands 1 and 3 where the third-order intermodulation frequency lands at the band 1 RX. The obtained RF measurement results show that the proposed method can efficiently suppress the nonlinear self-interference, while facilitating substantially lower computational complexity compared to the existing reference methods.

II. Proposed Digital Self-Interference Canceller

A. Nonlinear PIM Model

Let us first define an instantaneous basis function vector as

$$\boldsymbol{\phi}(n) = \begin{bmatrix} \phi_1(n) & \phi_2(n) & \cdots & \phi_C(n) \end{bmatrix}^T \tag{1}$$

where $\phi_i(n)$ denotes an individual basis function, and C is the total amount of basis functions. In this paper, for presentation convenience and practical applicability, we focus on the case of assuming 3rd-order nonlinear behavior in the individual band-specific PAs as well as a 3rd-order nonlinearity in the actual PIM stage. More elaborate scenarios with higher-order nonlinearities in the PAs and PIM interface are covered in our future extended work. The basis function vector $\boldsymbol{\phi}(n)$, forming the basis for nonlinear self-interference modeling at own RX

band, and thus its digital cancellation, reads now [6]

$$\boldsymbol{\phi}(n) = \begin{bmatrix} x_1(n)^2 x_2^*(n) \\ x_1(n)^2 x_2(n) x_2^*(n)^2 \\ x_1(n)^3 x_1^*(n) x_2^*(n) \\ x_1(n)^3 x_1^*(n) x_2(n) x_2^*(n)^2 \\ x_1(n)^4 x_1^*(n)^2 x_2^*(n) \\ x_1(n)^4 x_1^*(n)^2 x_2(n) x_2^*(n)^2 \end{bmatrix} \tag{2}$$

where $x_1(n)$ and $x_2(n)$ are the baseband equivalent signals of the two TX component carriers.

With the above assumptions, and accommodating different unknown relative weigths for the different basis function samples, represented as vector $\mathbf{g}_n$, the baseband equivalent nonlinear self-interference signal model at own RX reads

$$s(n) = \mathbf{g}_n^H \boldsymbol{\phi}(n). \tag{3}$$

To further allow for memory effects in the system, through a filter $\mathbf{w}_n$, the actual nonlinear PIM model is expressed as

$$y(n) = \mathbf{w}_n^H \mathbf{s}_n \tag{4}$$

where $\mathbf{s}_n = \begin{bmatrix} s(n+M_1) & \cdots & s(n-M_2) \end{bmatrix}$, M_1 is the number of pre-cursor memory taps, and M_2 is the number of post-cursor memory taps.

The complexity of the proposed decoupled canceller, i.e., in computing (2)–(4), is $(M_1 + M_2 + 1) + C$ complex multiplications per sample. The complexity of the reference canceller from [6], which adopts a linear-in-parameters model with independent filters for each basis function, is $(M_1+M_2+1)\times C$ complex multiplications per sample. The proposed solution thus yields a considerable reduction in modeling complexity particularly when considering higher-order PA and PIM nonlinearities. Additionally, as we show through RF measurements in Section III, very accurate PIM cancellation can still be obtained, despite the largely reduced complexity.

B. Cancellation and Decoupled Learning

Building on the above nonlinear model for the observable PIM, the signal after the digital cancellation is simply

$$e(n) = d(n) - y(n), \tag{5}$$

where $d(n)$ denotes the received signal. In practice, both the filters $\mathbf{g}$ and $\mathbf{w}$ are, however, unknown and must thus be estimated and possibly also tracked over time if there are time-dependent features in the involved nonlinearities.

For parameter learning and tracking, we define the cost function as $J(\mathbf{g}_n, \mathbf{w}_n) = |e(n)|^2$. Then, the corresponding gradient-based learning rule for the unknown parameter vector $\mathbf{g}$ reads

$$\mathbf{g}_{n+1} = \mathbf{g}_n - \mu_g \frac{\partial J(\mathbf{g}_n, \mathbf{w}_n)}{\partial \mathbf{g}_n}, \tag{6}$$

where μ_g is the learning step-size. After calculating the partial derivatives, the final learning rule can be expressed as

$$\mathbf{g}_{n+1} = \mathbf{g}_n + \mu_g e^*(n) \boldsymbol{\Phi}_n \mathbf{w}_n^*, \tag{7}$$

where $\boldsymbol{\Phi}_n = \begin{bmatrix} \boldsymbol{\phi}(n+M_1) & \cdots & \boldsymbol{\phi}(n-M_2) \end{bmatrix}$. It is noted that the learning rule for $\mathbf{g}$ depends on the other unknown filter $\mathbf{w}$.

As for learning the memory model $\mathbf{w}$, it can be noted that for given $\mathbf{g}$, the system is essentially identical to the classical least mean squares filter with $\mathbf{s}_n$ as the input signal, meaning that an LMS-like learning rule can be adopted. Therefore, the learning rule for $\mathbf{w}_n$ is written as

$$\mathbf{w}_{n+1} = \mathbf{w}_n + \mu_w e^*(n) \mathbf{s}_n, \tag{8}$$

where μ_w is the memory step size. These learning rules are executed in parallel such that both $\mathbf{g}$ and $\mathbf{w}$ are updated simultaneously using the values from the previous iteration.

C. Self-orthogonalized Learning for Faster Convergence

Due to the mutual correlation between the nonlinear basis functions in $\boldsymbol{\phi}(n)$, the learning rule in (7) may suffer from slow convergence. To address this, a self-orthogonalizing learning rule can be used instead. Inspired by [7, p. 356], the filter input vector is expressed as $\mathbf{u}_n = \boldsymbol{\Phi}_n \mathbf{w}_n^*$, and the self-orthogonalizing learning rule can be expressed as

$$\mathbf{g}_{n+1} = \mathbf{g}_n + \tilde{\mu}_g \mathbf{R}^{-1} e^*(n) \mathbf{u}_n, \tag{9}$$

where $\tilde{\mu}_g$ is the step size, and $\mathbf{R} = \mathrm{E}\left[\mathbf{u}_n \mathbf{u}_n^H\right]$ is the correlation matrix of the filter input vector.

Assuming then that the baseband signals of the two transmit carriers are independent and identically distributed (i.i.d.) and stationary, the correlation matrix $\mathbf{R}$ can be easily expressed, for given $\mathbf{w}$, as

$$\mathbf{R} = \mathbf{R}_{\boldsymbol{\phi}} \mathbf{w}_n^H \mathbf{w}_n, \tag{10}$$

where $\mathbf{R}_{\boldsymbol{\phi}}$ is the correlation matrix of the basis functions. Note that $\mathbf{R}_{\boldsymbol{\phi}}$ is only based on the chosen signal model and the statistical properties of the utilized waveforms, meaning that it can be calculated offline, alongside with its inverse. Thus, we can rewrite the self-orthogonalizing learning rule as

$$\begin{aligned} \mathbf{g}_{n+1} &= \mathbf{g}_n + \frac{\tilde{\mu}_g}{\mathbf{w}_n^H \mathbf{w}_n} \mathbf{R}_{\boldsymbol{\phi}}^{-1} e^*(n) \mathbf{u}_n \\ &= \mathbf{g}_n + \mu_{g,\mathrm{ort}} \mathbf{R}_{\boldsymbol{\phi}}^{-1} e^*(n) \boldsymbol{\Phi}_n \mathbf{w}_n^*, \end{aligned} \tag{11}$$

where $\mu_{g,\mathrm{ort}}$ is the final step size. Note that, as a simplification, the step size can be chosen to be static, despite the time-variant term $\mathbf{w}_n^H \mathbf{w}_n$. Therefore, the only additional computation required in this learning rule, opposed to that in (7), is the matrix multiplication since $\mathbf{R}_{\boldsymbol{\phi}}^{-1}$ can be precomputed.

III. RF Measurement Results and Analysis

The performance of the proposed digital self-interference canceller is now evaluated through practical RF measurements. The experimental setup builds on the Analog Devices AD9368 2x1 transceiver board for generating the LTE/NR Band 1 and Band 3 uplink CCs, followed by commercial UE RF modules. Each TX CC is amplified separately using Skyworks multiband PA modules (SKY77643-21), combined in a dual-band multiplexer (TDK B8960), and finally fed to an antenna switch (BGS12PL6). The output RF port of the switch is connected to a wideband mobile antenna. As discussed in the

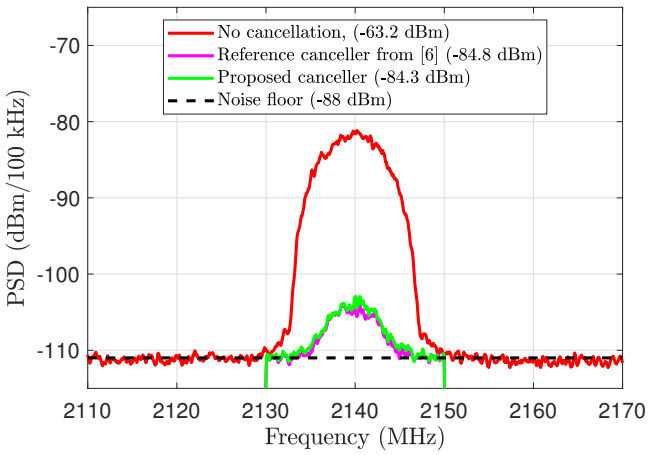

Fig. 1: Measured PIM at Band 1 receiver with and without digital cancellation. The TX power is +24 dBm.

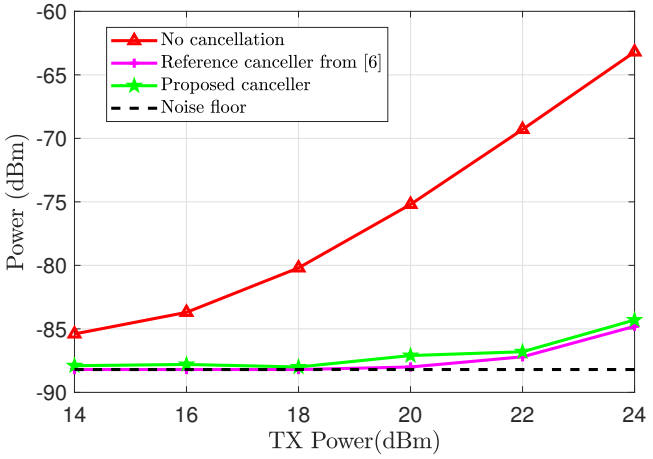

Fig. 2: The measured residual noise+PIM power, with and with digital cancellation, as a function of TX power.

introduction, intermodulation of the transmit carriers leads to self-interference at Band 1 receiver, which is observed and measured at Band 1 receiver port of the multiplexer using a National Instruments vector signal transceiver (VST, PXIe5645R). The VST downconverts and digitizes the signal to baseband, and the digital samples are read from the VST memory and loaded into host processor for post-processing and algorithm evaluation. All the measurements are carried out in an electromagnetic compatibility (EMC) chamber to minimize the impact of external interference signals. For algorithm evaluation, the bandwidths of the TX CCs are assumed to be 5 MHz, each, and the filter $\mathbf{w}_n$ has $M_1 = 3$ pre-cursor and $M_2 = 4$ post-cursor taps, while $C = 6$.

Fig. 1 shows the essential power spectral density (PSD) curves before and after digital cancellation with the full aggregated transmit power of +24 dBm. Here, for illustration purposes, x-axis ticks are deliberately labeled as the actual receiver RF frequencies even though the actual processing is done at digital baseband. Firstly, one can observe the substantial level of the PIM-induced self-interference when employing commercial RF components, which can cause receiver desensitization. Secondly, the proposed decoupled-learning based canceller is able to efficiently suppress the self-interference by more than 21 dB, and is capable of achieving almost identical cancellation performance as the reference canceller from [6] with much lower complexity. Specifically, the proposed and reference cancellers need $(M_1+M_2+1)+C = 14$ and $(M_1 + M_2 + 1) \times C = 48$ complex multiplications, respectively, per cancelled sample.

The performance is further assessed by plotting the noise plus self-interference power at Band 1 with respect to different TX power levels, with and without digital cancellation, in Fig. 2. Here, it is interesting to note that the self-interference is already noticeable even at lower TX powers, which can cause receiver sensitivity degradation. The proposed digital cancellation approach is again shown to sufficiently suppress the self-interference such that system noise floor is not heavily degraded, and can thus extend the usable transmit power range.

One can also observe that at highest transmit powers, there is still some residual PIM. These are likely to be stemming from higher-order nonlinear terms and PA memory effects, thus developing advanced cancellation techniques for their mitigation is addressed in our future work.

Conclusion

In this paper, we proposed a novel reduced complexity digital self-interference cancellation algorithm, to mitigate the co-existing PA and PIM induced nonlinearities in FDD transceivers. The proposed technique reduces the computational complexity during the parameter learning in comparison to state-of-the-art linear-in-parameters cancellers. The RF measurement results in LTE/NR Bands 1 and 3 carrier aggregation context demonstrated up to 21 dB suppression of the self-interference. Implementing such algorithms in radio transceivers will enable extending their usable transmit power range, and possibly also relaxing the linearity requirements of the RF components. Our future work will focus on extending the algorithms to incorporate higher-order nonlinearties.

References

[1] E. Dahlman, S. Parkvall, and J. Sköld, *5G NR: the Next Generation Wireless Access Technology*. Academic Press, 2018.

[2] 3GPP Tech. Spec. 36.101, "LTE Evolved Universal Terrestrial Radio Access (E-UTRA) User Equipment (UE) radio transmission and reception," v16.1.0 (Release 16), April 2019.

[3] 3GPP Tech. Spec. 38.101-1, "NR User Equipment (UE) radio transmission and reception; Part 1: Range 1 Standalone," v15.5.0 (Release 15), April 2019.

[4] H. T. Dabag, H. Gheidi *et al.*, "All-digital cancellation technique to mitigate receiver desensitization in uplink carrier aggregation in cellular handsets," *IEEE Trans. Microw. Theory Tech.*, vol. 61, no. 12, pp. 4754–4765, Dec. 2013.

[5] M. Z. Waheed, P. P. Campo *et al.*, "Digital cancellation of passive intermodulation in FDD transceivers," in *2018 52nd Asilomar Conference on Signals, Systems, and Computers*, Oct. 2018, pp. 1375–1381.

[6] M. Z. Waheed, D. Korpi *et al.*, "Digital self-interference cancellation in inter-band carrier aggregation transceivers: Algorithm and digital implementation perspectives," in *2017 IEEE International Workshop on Signal Processing Systems (SiPS)*, Oct. 2017, pp. 1–5.

[7] S. Haykin, *Adaptive Filter Theory*, 4th ed. Prentice Hall, 2002.